

INFLUENCE OF PROCESS PARAMETERS DURING PLASMA ARC WELDING PROCESS OF INCONEL 718

B. CHINNA ANKANNA *

Research Scholar, Department of Mechanical Engineering, Jawaharlal Nehru Technological University Anantapur, Ananthapuramu, Andhra Pradesh, India.

Working at RGM CET, Nandyal, Andhra Pradesh, India.

*Corresponding Author Email: ankanna.jntuaphdscholar@gmail.com

K. GOVINDARAJULU

Professor, Department of Mechanical Engineering, Jawaharlal Nehru Technological University Anantapur College of Engineering, Ananthapuramu, Andhra Pradesh, India. Email: govindjntu@gmail.com

Abstract

The demand for high quality alloyed joints in aviation, automotive and power generative domain have led to the evolution of plasma arc welding process. In fact, nickel based super alloys is one such element that serves the purpose due to its extraordinary combination of high strength, oxidation and corrosion resistant properties even at extreme service conditions. However, fusion welding of Inconel 718 alloy is often associated with solidification cracking and fissure formation which challenges its weldability. Therefore, the present work is focused on presenting a detailed investigation on the influence of processing conditions on weld quality characteristics of Inconel 718 alloy. The design of experiments is framed such that the gas flow rate, welding speed along with current is varied for a constant arc voltage during plasma arc welding of Inconel 718 alloy. The processing conditions are varied in order to evaluate the macro and microstructural features along with micro-hardness attribute. Based on macro microstructural features and hardness attribute it can be assessed that plasma welding have immense potential to weld Inconel alloy without generating any major defects such as spatter, cracks, gas holes or porosity and it can be recommended for industrial application.

Keywords: Plasma arc Welding, Inconel 718 Alloy, Microstructure, Hardness.

1. INTRODUCTION

The inclination towards nickel based super alloys is growing steadily over time for the manufacture of critical components in aviation, power generating and automobile industries. Inconel 718 alloy belong to austenitic Ni-Fe super alloy parent metal. Moreover, it has excellent oxidation and corrosion resistant property that can serve at extreme climatic conditions [1] and exhibits high strength over a temperature range of -250 °C to 650 °C. Also, this super alloy exhibits high tensile strength, good fatigue strength and creep resistance behavior. This property enables its application in the areas of aircraft turbine and nuclear reactor parts over aluminium, steel and other super alloys.

In fact, fusion welding is the most widely opted procedure in manufacturing industries due to freedom of joining different range of similar and dissimilar metals, lower operating cost, higher production rate and efficiency. It is primarily melting of base metal with an intense thermal energy source followed by solidification and not much alteration in material attributes. The most distinguishable parameter that differentiates each of these fusion welding processes is the heat intensity factor that will determine weld joint integrity. A

lower heat input results in structural and metallurgical inhomogeneity while a higher heat input leads to keyhole formation and lower heat conduction from melt pool to base metal region. Joining of plates by conventional arc welding processes induces undesirable outcomes such as residual stresses, distortion and microstructural inhomogeneity. Therefore, to essentially eliminate nonuniformity in welded part proper welding process has to be selected. And, plasma arc welding process is one such welding method which utilises high focused thermal energy to join metal elements and super alloys and produces narrow weld bead and minimum HAZ.

In the past few decades, researches is primarily focused towards issues associated with joining of Inconel 718 alloy using different welding approaches. Inconel 718 alloy has greater than 20 primary and secondary alloy elements. The primary alloy elements included in the super alloy for solid strengthening are Mo, Cr, Fe and Co. The radii of these elements are much more similar to that of nickel and this super alloy is subjected to development of secondary intermetallic elements during welding process on account of presence of more number of alloying elements. And, one of the common phenomena is segregation of heavy elements and mismatch of atomic radii during the solidification process [2]. Therefore, proper control of growth and alloy elements segregation at the grain boundary is critically vital in terms of strength aspect. The major constraint to fabricate this super alloy is crack generation and formation of fissures at micro scale level in the weld and heat affected areas. The underlying cause to these defects are segregation of alloying elements at the interdendritic region and this eventually results in formation of metal carbides and brittle intermetallic phases. Therefore, it can be assessed that the distribution and fraction of intermetallic phases significantly affects the structural attributes of alloy and at times leads to early failure of the component during the service life [3]. In fact, a number of comparative analysis was carried out between different welding methods such as laser beam welding (LBW), electron beam welding (EBW) and gas tungsten arc welding (GTAW) in order to assess the more feasible welding method for Inconel 718 alloy [4-8].

The percentage content of intermetallic phases and segregation at the interfacial region of weld and heat affected zone was determined to be factor of thermal energy input and solidification rate. Advanced joining techniques were determined to have beneficiary effects on microstructural evolution and structural attributes of welded specimen on account of controlled and regulated heat input. This yields higher solidification rate when compared with conventional joining processes. Radhakrishna and Rao examined the segregational behavior in gas tungsten arc and electron beam welded Inconel 718 alloy specimens [9]. The tendency of undesirable phase formation is higher in GTAW specimen than EBW specimen due to high heat input delivery and lower solidification rate. The lower content of undesirable phases at interfacial region have relatively enhanced the creep resistance property in EBW samples. The crack development at the weld zone is due to constitutional liquation of Nb rich carbide in gas tungsten arc welded specimens [10]. The authors compared the microstructural features with CO₂ laser and Nd-YAG pulsed laser sources with reference to thermal energy input and solidification rate [11]. It was recognised that the dendritic arm spacing reduces with increase in thermal energy

input. This in effect produces fine micro-structure and hinders the development of intermetallic phases and segregation at the grain boundary. Janaki Ram et al. concluded that refined grain morphology and lower percentage of intermetallic phases can be obtained by minimising thermal energy input and improving solidification rate [12]. Apparently, with this approach not only structural attribute is improved but also post weld heat treatment response is significantly improved. Thavamani et al. pointed out that crack sensitivity along with dendritic arm spacing can be reduced by incorporating ultrasonic vibration during GTAW process of Inconel 718 alloy [13].

The high heat input delivery to the base metal results in non-uniform temperature gradient across the specimen. This eventually leads to non-homogenous grain evolution and other undesirable stress generation and deformation in the weldment. Therefore, proper post-welding heat treatment procedures has to be followed to reduce the non-homogeneity across the welded specimen [14-17]. Inconel 718 alloy has the tendency to solidify in the dendritic approach over a wide temperature range during the joining procedure. Thereby, vital alloying elements such as Ti, Mo and Nb will segregate and transpire in the weld area and presence of primary alloy elements in the inter-dendritic domain during the solidification process will affect the structural attributes of the weldment. Although, the presence of intermetallic structures such as Laves in the weld area will result in undesirable structural attributes [18] and obstructs the precipitation of principal strengthening elements γ^I and γ^{II} in the metal matrix. Besides, few strengthening phases such as intergranular δ elements are generated in the weld area which obstructs the grain sliding during loading condition. Although, lower melting point of intermetallic phases in the weld domain will initiate crack formation and result in early failure of the component [19-21].

Based on existing literature, it was determined that a thorough study on weld quality characteristics and attributes of Inconel 718 alloy especially using plasma arc welding process is not explored yet. And, the current investigation is focused towards this direction whereby, the weld morphology and attributes of nickel based super alloy is distinguished using key weld parameters. A proper study on the effects of weld variables on Inconel 718 alloy is intended to analyse and comprehend the interaction of plasma arc with base metal and evolution of distinct zones in weldment during the process.

2. MATERIAL AND METHODS

In PAW, the thermal energy of constricted plasma arc is employed for joining and fabrication which is produced by coalescence of plasma ions. The principal operating modes of PAW process are melt-in mode and keyhole mode. These operating modes is governed and controlled by the input arc current parameter. The principal operating parameters of PAW process which will determine the weld integrity are arc voltage, plasma current, weld velocity and flow rate of inert gas. The benefit of PAW over traditional arc joining processes is the arc stability which provides higher accuracy in terms of joining of plates. The experimental set-up of PAW process is presented in Figure 1. The experiments are carried out using plasma arc welding machine and the polarity of

electrode is negative viz. DCEN mode. The work pieces are clamped on restrained fixture mounted over work table and the fixture is made of stainless steel in order to arrest all degrees of freedom and achieve high cooling rate. The plasma torch is moved over the rail guided platform. Commercial pure argon gas of 99.99% purity and flow rate of shielding gas is maintained at 10 LPM and 12 LPM is maintained. A thoriated tungsten electrode is employed of 1 mm diameter and a 2 mm stand-off distance is maintained for all the processing conditions.



Figure 1: In house developed plasma arc welding experimental setup

Inconel 718 alloy plates of 3 mm thickness is used to produce autogenous welds in butt joint configuration. The microstructure of base metal Inconel 718 alloy is presented in Figure 2. It comprises of equi-axed grains of diameter 72 μm . The compositional elements of base metal are obtained by wet analysis and it is presented in Table 1. Al, Cr and Si provides oxidation resistant property in super alloy while Nb provide strength to Inconel 718 alloy. Other elements such as Ti, Mo, C in nickel based super alloy have the tendency of precipitation at the boundary region and decline the possibilities of boundary slipping effect.

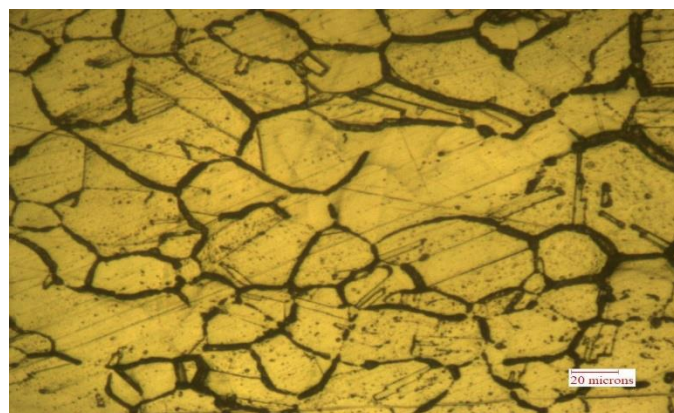


Figure 2: Grain structure of Inconel 718 alloy base metal

Table 1: Chemical composition of Inconel 718 in weight %

Element	Wt.%	Element	Wt.%
Cr	18.2	S	0.006
Nb+Ta	5.19	P	0.005
Mo	3.15	Fe	Balance
Ti	1.02	B	0.005
Al	0.48	Cu	0.02
Si	0.07	Co	0.02
C	0.027	Ni	53
Mn	0.07		

Welding of Inconel 718 alloy plates were carried out by carefully selecting processing variables. Since, insufficient heat input may result in partial or incomplete penetration and excessive thermal energy may lead to burn out of the base metal. Therefore, heat input has to be properly selected for welding operation. Initially few bead-on-plate experiments were carried out to stabilise the operating parameters thereafter, design of experiments were framed for different processing conditions of PAW process. In the present investigation, welding current, velocity, gas flow rate were varied for a constant arc voltage. The welding current was varied from 75 A to 105 A and welding speed was maintained at four different levels viz, 2.5 mm/s, 3 mm/s, 3.5 mm/s and 4 mm/s. The gas flow rate was adjusted between 10 LPM and 12

LPM while the arc voltage was maintained constant at 20V for all the processing conditions.

Table 2: Plasma arc welding process parameters for Inconel 718

Data Set No.	Current (A)	Welding Velocity (mm/s)	Gas Flow Rate (LPM)	Voltage (V)
1	75	2.5	12	20
2	85	2.5	12	20
3	95	2.5	10	20
4	105	2.5	10	20
5	75	3	12	20
6	85	3	12	20
7	95	3	10	20
8	105	3	10	20
9	75	3.5	12	20
10	85	3.5	12	20
11	95	3.5	10	20
12	105	3.5	10	20
13	75	4	12	20
14	85	4	12	20
15	95	4	10	20
16	105	4	10	20

For analysing the grain structures of welded Inconel 718 alloy, Carpenter's stainless steel etch solution was employed and its composition is 2.125 g FeCl₃, 0.6 g of CuCl₂, 30.5 mL of C₂H₂OH, 30.5 mL of HCl and 1.5 mL of HNO₃. The microstructural features were recognised and observed using optical microscopy for different resolutions. The hardness at different sections of welded sample were measured using Vickers micro-hardness testing machine. The indentations were made at an interval of 1 mm in transverse direction using an indentation load of 500 kgf for each indentation. The load was applied for 5s at specific locations and thereafter the microhardness magnitude was obtained from the test dial indicator.

3. RESULTS AND DISCUSSION

The weld surface appearance of butt jointed Inconel 718 alloy corresponding to data set #14 is presented in Figure 3. It can be recognised that a smooth weld bead is obtained on account of incorporation of constant heat flux during the process of continuous mode plasma arc welding. The melting and solidification duration of metal alloy is closely associated with heat flux and weld velocity. In fact the morphology of weldment is varying corresponding to different weld variables. It has been determined that with an increase in arc current, the weld width increased which led to an increased weld dimension. However, in the present study the weld surface appearance of Inconel 718 alloy cannot be distinguished much with an increase or decrease in weld velocity and flow rate of inert gas. Since, the variation of weld velocity and flow rate magnitude is nominal when compared with arc current. Moreover, from the developed joint and surface appearance it can be assessed that the overall characteristics of butt jointed Inconel 718 alloy plates is sound.

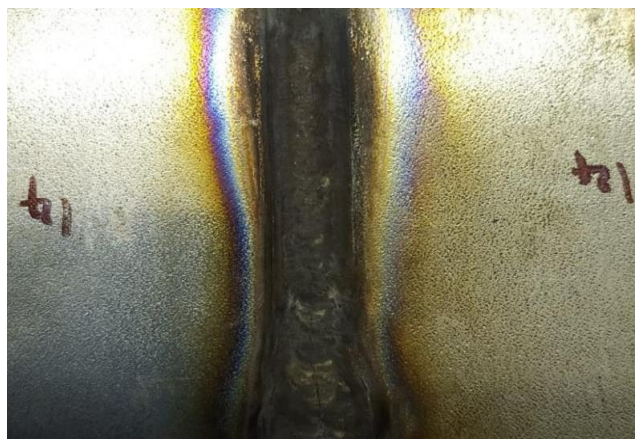


Figure 3: Top surface appearance of Inconel 718 joint welded by plasma arc welding corresponding to arc current of 85 A, gas flow rate of 12 LPM and 4 mm/s welding speed

Figure 4 presents the weld macrograph of nickel super alloy corresponding to welding condition #3 of Table 2. The optical macrostructure reveals that cracks or pores are not present in the weld and heat affected zone. This confirms that the flow rate of shielding

gas during the process is efficient in overcoming weld defects for the continuous mode plasma arc welding process and a sound weld joint is obtained. The weld width and penetration is determined as 7.98 mm and 2.15 mm respectively. Moreover, the weld profile is hemispherical and wider which supports the fact that conduction or melt-in mode welding is carried out for the specified processing condition. Moreover, a uniform weld profile is recognised across the butt aligned plates which demonstrates the fact that equal proportion of parent metal is being melted and solidified due to constricted and narrow plasma beam. Although, the heat affected zone (HAZ) is determined to be narrow and brighter in colour than the base metal region.

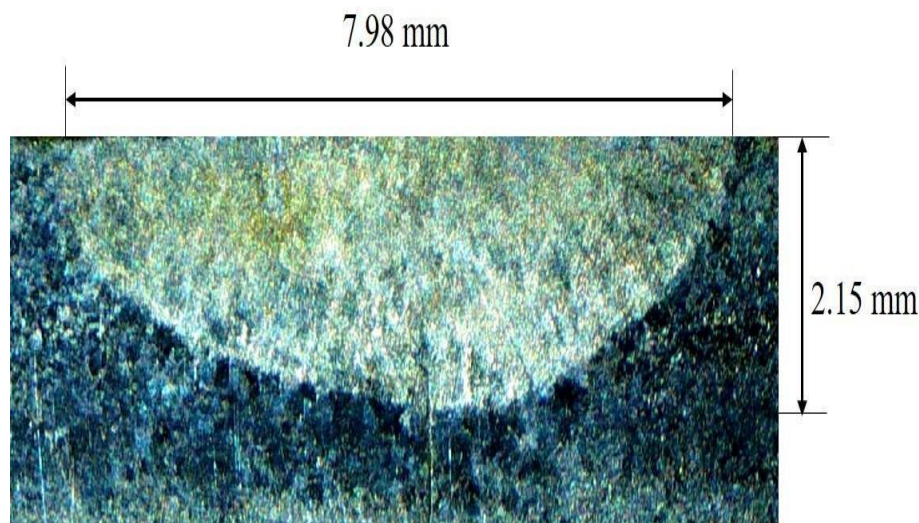


Figure 4: Macrostructure of Inconel 718 alloy corresponding to an arc current of 95 A, welding speed of 2.5 mm/s and gas flow rate of 10 LPM

The comparison of Inconel 718 alloy weld macrographs are presented in Figure 5 for different processing conditions provided in Table 2. The butt joining of Inconel 718 alloy transpires at two distinct weld velocities and for the same processing conditions of arc current, shielding gas flow rate and arc voltage. It can be identified from the macrographs that the weld penetration is relatively lower at lower welding velocity when compared with higher welding velocity. With an increase in welding, the weld penetration was enhanced relatively due to higher heat input delivery in shielding gas environment. Moreover, it is recognised that the weld profile is dumb-bell shaped for data set condition #2 and #6 as against data set condition #3 and #11 which is almost hemispherical shaped. Although, the weld profile is more hemispherical and symmetric across the weld joint at 75 A than other two processing conditions. This demonstrates that the arc current has a significant role in determining the weld profile instead of weld velocity and shielding gas flow rate. The profile fluctuated between hemispherical and dumb-bell shaped with an increase in arc current. This also signifies that arc current influences the physical parameters such as Marangoni number and Peclet number which will determine the overall geometry and profile of the weldment.

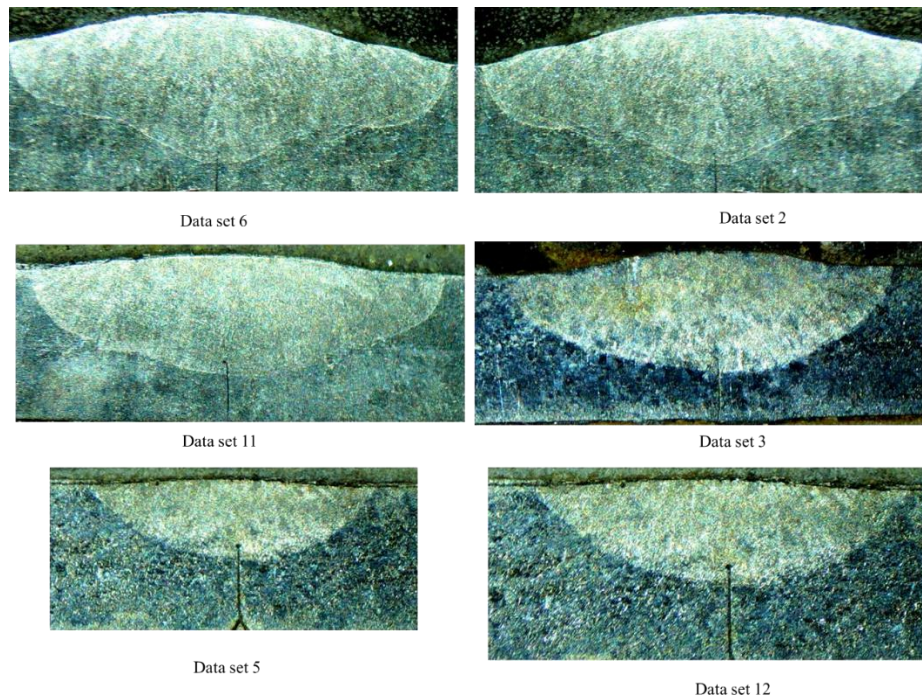


Figure 5: Comparison of weld macrographs with respect to processing condition provided in Table 2

The microstructure of Inconel 718 alloy at different locations is presented in Fig.6. The base metal region is identified by a uniform distribution of austenitic structures which is also associated with strength. The HAZ width is very narrow which also confirms the plasma arc is confined to a very small region. Moreover, the grains are dense and coarse in the HAZ region when compared with the base metal region. And, the grains in the HAZ is identified with carbides. Although, the weld region exhibits elongated dendritic structures which are evolved due to moderate cooling rate.

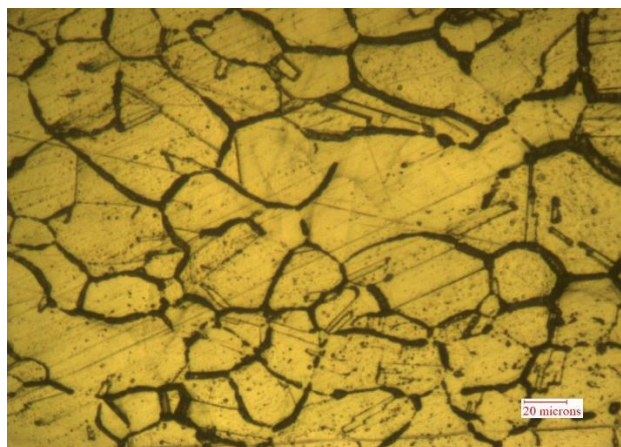


Figure 6: Parent material (Inconel 718) microstructure after welding process was performed

Figure 6 depict the microstructure of parent material zone after welding experiment was carried. This microstructure is related to experimental process variables data set 1 given in table 2. The grain structures of Inconel 718 present the existence of MC-type carbides which is distributed in the matrix. Figure 7 describes the microstructure of weld zones viz. heat affected and weld zones for data set 1 of table 2. From this figure it can be recognised that the variation of grain size and structure with respect to parent material.

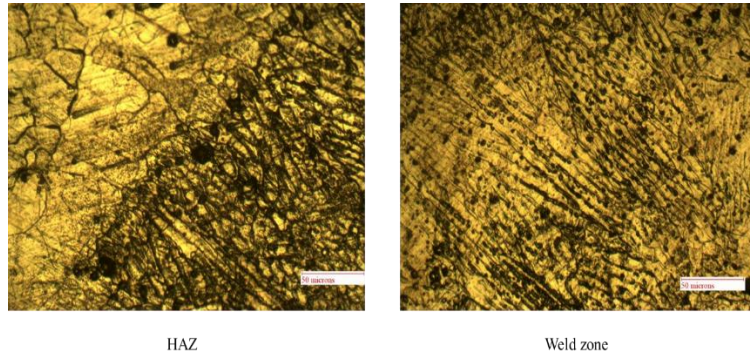


Figure 7: Micrograph of Inconel 718 weld of different zone corresponding to processing conditions (data set 1) of table 2

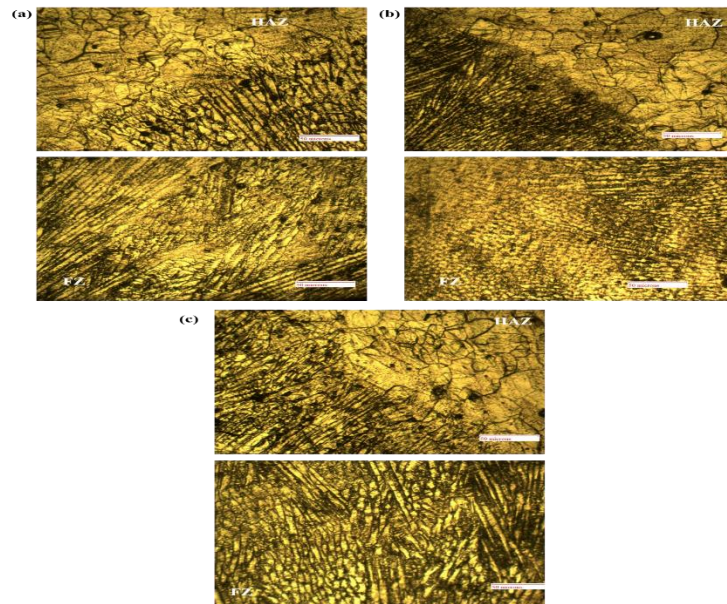


Figure 8: Microstructures of weld cross-sections of Inconel 718 corresponding to welding conditions given in table 2 (a) data set 4, (b) data set 12 and (c) data set 16

At an elevated peak temperature with reference to higher thermal energy input, the weld pool remains for a protracted time period. This in effect increases the solidification time and leads to a coarser grain evolution. From the micrographs it is detected that equiaxed dendrites and multidirectional columnar grains are present in the solidified zone.

Moreover, dendrites of columnar morphology are majorly determined near the boundary region. In fact refine cellular and equiaxed dendrites are observed at the centre of the weld zone and it is in the low temperature gradient zone. The high-magnification micrograph (in figures 8) indicates the development of coarse uninterrupted intermetallic elements of columnar morphology in interdendritic region when compared with the equiaxed structure. Figures 8 shows different zones (fusion and heat affected areas) of plasma arc welds of Inconel 718 for different welding conditions of table 2. In figures 8 (a), (b) and (c), the weld interface between weld and heat affected areas can be observed.

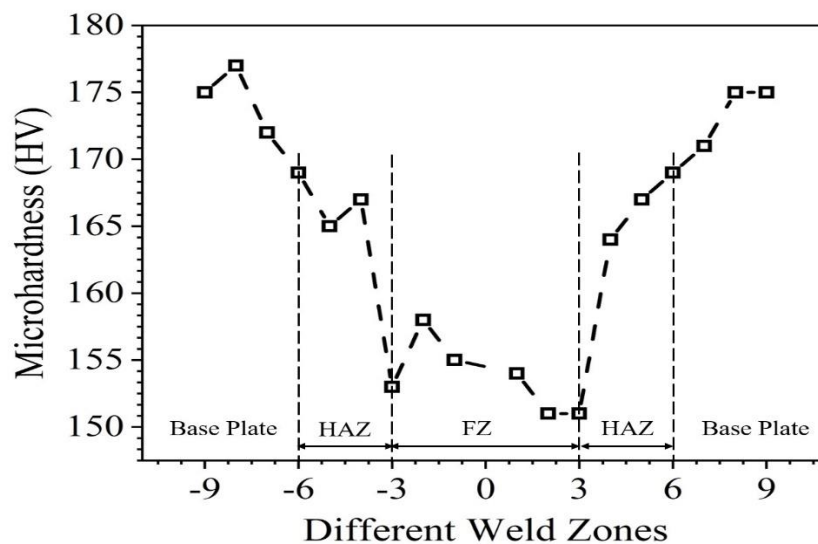


Figure 9: Vickers's microhardness profile across weld cross-section corresponding to data set 1 of table 2

After examining the metallographic analysis (macro and microstructures), microhardness distribution was estimation for parent material and two different weld zones (FZ and HAZ). Figure 9 depict the microhardness distribution corresponding to data set 1 of table 2 in parent metal and other weld zones. The average hardness of the base metal is 178 ± 2 HV for the Inconel 718. The hardness value in the fusion zone marginally falls for Inconel 718 and this is primarily due to migration of the principal alloying elements such as Nb, Ni, and Mo from the Inconel 718 base metal.

4. CONCLUSION

The present work is focused on presenting a suitable process window range for welding Inconel 718 alloy using plasma arc joining process. This welding approach is highly recommendable since overall production cost is much lower than laser and electron beam welding process. The following summary may be derived from the present work:

- ❖ A detailed experimental investigation was carried out for the joining of Inconel 718 using plasma arc welding technique. In the course of investigation, the process

variables welding current, shielding gas flow rate and welding velocity was examined with respect to metallographic analysis and mechanical properties.

- ❖ From the present work, it is observed that gas flow rate has significant influence on weld attributes and structural features.
- ❖ The grain structures at distinct weld zones has influence on hardness property. The hardness at weld and heat affected zone is higher than the base metal.
- ❖ At an elevated thermal energy input, the average cooling rate reduces and results into the coarser solidification structure and comparatively lower mechanical properties.
- ❖ With a rise in thermal energy input, the average hardness value in the fusion zone reduces. Overall, with an average heat input results in significant refinement of the weld microstructure.

Ethics Declarations

The authors declare that they have no conflict of interest.

Acknowledgements

The authors would like to acknowledge the Department of Mechanical Engineering, Jawaharlal Nehru Technological University Ananthapuramu, Andhra Pradesh, India in all aspect to carry out the present work.

References

- 1) Henderson MB, Arrell D, Larsson R, Heobel M, Marchant G, Nickel based superalloy welding practices for industrial gas turbine applications. *Sci. Technol. Weld. Join* **9**: 13–21 (2004). <https://doi.org/10.1179/136217104225017099>
- 2) Manikandan SGK, Sivakumar D, Rao KP, Kamaraj M, Effect of weld cooling rate on Laves phase formation in Inconel 718 fusion zone. *J. Mater. Process. Technol* **214**: 358–364 (2014). <https://doi.org/10.1016/j.jmatprotec.2013.09.006>.
- 3) Huang CA, Wang TH, Lee CH, Han WC, A study of the heat-affected zone (HAZ) of an Inconel 718 sheet welded with electron-beam welding (EBW). *Mater. Sci. Eng A* **398**: 275–281 (2005). <https://doi.org/10.1016/j.msea.2005.03.029>.
- 4) Baruah M, Bag S, Influence of heat input in microwelding of titanium alloy by micro plasma arc. *J. Mater. Process. Technol* **231**: 100–112 (2016). <https://doi.org/10.1016/j.jmatprotec.2015.12.014>.
- 5) Cao X, Rivau B, Jahazi M, Cuddy J, Birur A, Effect of pre- and post-weld heat treatment on metallurgical and tensile properties of Inconel 718 alloy butt joints welded using 4 kW Nd:YAG laser. *J Mater Sci* **44**: 4557–4571 (2009). <https://doi.org/10.1007/s10853-009-3691-5>.
- 6) Chen HC, Pinkerton AJ, Li L, Fibre laser welding of dissimilar alloys of Ti-6Al4V and Inconel 718 for aerospace applications. *The International Journal of Advanced Manufacturing Technology* **52**: 977–987 (2011).
- 7) Janaki Ram GD, Venugopal Redd A, Prasad Rao K, Madhusudhan Reddy, Control of Laves phase in Inconel 718 GTA welds with current pulsing. *Science and Technology of welding and joining* **9**: 390–398 (2004).

- 8) Ram GDJ, Reddy AV, Rao KP, Redd GM, Microstructure and mechanical properties of Inconel 718 electron beam welds. *Materials Science and Technology* **21**: 1132– 1138 (2005). <https://doi.org/10.1179/174328405X62260>.
- 9) Radhakrishna C, Rao KP, Studies on creep/stress rupture behaviour of superalloy 718 weldments used in gas turbine applications. *Materials at high temperatures* **12**: 323–327 (1994).
- 10) Knorovsky GA, Cieslak MJ, Headley J, Romig D, Hammetter WF 1989 INCONEL 718: A solidification diagram. *Metall. Trans A* **20**: 2149–2158. <https://doi.org/10.1007/BF02650300>.
- 11) Gobbi S, Zhang L, Norris J, Richter KH, Loreau JH, High powder CO₂ and Nd YAG laser welding of wrought Inconel 718. *Journal of Materials Processing Technology, International Conference on Advances in Material and Processing Technologies* **56**: 333–345 (1996). [https://doi.org/10.1016/0924-0136\(95\)01847-6](https://doi.org/10.1016/0924-0136(95)01847-6).
- 12) Janaki Ram GD, Venugopal Reddy A, Prasad Rao K, Reddy GM, Sarin Sundar JK, Microstructure and tensile properties of Inconel 718 pulsed Nd-YAG laser welds. *Journal of Materials Processing Technology* **167**: 73–82 (2005). <https://doi.org/10.1016/j.jmatprotec.2004.09.081>.
- 13) Thavamani R, Balusamy V, Nampoothiri J, Subramanian R, Ravi KR, Mitigation of hot cracking in Inconel 718 superalloy by ultrasonic vibration during gas tungsten arc welding. *Journal of Alloys and Compounds* **740**: 870–878 (2018). <https://doi.org/10.1016/j.jallcom.2017.12.295>.
- 14) Ram GDJ, Reddy AV, Rao KP, Reddy GM, Microstructure and mechanical properties of Inconel 718 electron beam welds. *Materials Science and Technology* **21**: 1132– 1138 (2005). <https://doi.org/10.1179/174328405X62260>.
- 15) Gobbi S, Zhang L, Norri J, Richter KH, Loreau JH, High powder CO₂ and Nd YAG laser welding of wrought Inconel 718. *Journal of Materials Processing Technology, International Conference on Advances in Material and Processing Technologies* **56**: 333–345 (1996). [https://doi.org/10.1016/0924-0136\(95\)01847-6](https://doi.org/10.1016/0924-0136(95)01847-6).
- 16) Madhusudhana Reddy G, Srinivasa Murthy CV, Srinivasa Rao K, Prasad Rao K, Improvement of mechanical properties of Inconel 718 electron beam welds—influence of welding techniques and post weld heat treatment. *Int J Adv Manuf Technol* **43**: 671–680 (2009). <https://doi.org/10.1007/s00170-008-1751-7>
- 17) Thompson RG Dobbs R Mayo DE, The Effect of Heat Treatment on Microfissuring in Alloy 718. *Weld. J.* **65**: 299 (1986).
- 18) Mei Y, Liu Y, Liu C, Li C, Yu L, Guo Q, Li H, Effect of base metal and welding speed on fusion zone microstructure and HAZ hot-cracking of electron-beam welded Inconel 718. *Materials & Design* **89**: 964–977 2016. <https://doi.org/10.1016/j.matdes.2015.10.082>.
- 19) Ma D, Response of primary dendrite spacing to varying temperature gradient during directional solidification. *Metallurgical and Materials Transactions B* **35**: 735–742 (2004).
- 20) Phillips PJ, McAlliste D, Gao , Lv D, Williams REA, Peterson B, Wang Y,
- 21) Mills M, Nano γ'/γ " composite precipitates in Alloy 718. *Appl. Phys. Lett* **100**: 211913 (2012). <https://doi.org/10.1063/1.4721456>.
- 22) Kuo C-M, Yang Y-T, Bor H-Y, Wei C-N, Tai C-C, Aging effects on the microstructure and creep behavior of Inconel 718 superalloy. *Materials Science and Engineering: A, 11th International Conference of Creep and Fracture of Engineering Materials and Structures, CREEP 2008* 510–511, 289–294 (2009). <https://doi.org/10.1016/j.msea.2008.04.097>.